



Monthly Bulletin

Institut de physique du globe de Paris
Observatoire volcanologique du Piton de la Fournaise

ISSN 2610 – 5101

April, 2026

PITON DE LA FOURNAISE (VNUM #233020)

Latitude: 21.244°S

Longitude: 55.708°E

Summit elevation: 2632 m

Piton de la Fournaise is a basaltic hot spot volcano located in the southeastern part of La Réunion Island (Indian Ocean). The volcano first erupted about 500,000 years ago. Its volcanic activity is characterized by frequent effusive eruptions (with emissions of lava fountains and lava flows) that occur on average twice a year since 1998. More rarely, larger explosive eruptions (with blocks covering the summit area and ash emissions that can disperse over long distances) have happened in the past with a centennial recurrence rate.

Most of the current eruptive activity (97% during the last 300 years) occurs from vents inside the Enclos Fouqué caldera. A few eruptions, however, have occurred from vents outside the caldera (most recently in 1977, 1986, and 1998). Such eruptions can potentially threaten communities that live in the surrounding areas.

Since late 1979, the activity of Piton de la Fournaise is monitored by the Piton de la Fournaise Volcanological Observatory (Observatoire Volcanologique du Piton de la Fournaise - OVPF), which belongs to the Institut de Physique du Globe de Paris (IPGP).

Alert level: Alert 2-2
(from March, 12 to May, 5 2026)

(cf. table in the appendix)



A. Piton de la Fournaise activity

The eruption that began on February 13, 2026 (06:00 UTC) ended on April 12, 2026 (19:10 UTC). A total of three active phases were observed, interspersed with two inactive phases during which no surface activity occurred:

- . between March 25 (12:30 UTC) and March 28 (11:00 UTC),
- . and between April 2 (20:10 UTC) and April 8 (9:15 UTC) (see Section B for more details).

Three phases of tremor without eruptive activity were also recorded during the second pause and following the end of the eruption:

- . from April 3 (4:40 p.m. UTC) to April 8 (9:15 a.m. UTC),
- . from April 14 (11:00 a.m. UTC) to April 15 (7:20 a.m. UTC),
- . and from April 19 (2:20 a.m. UTC) to April 21 (12:10 p.m. UTC).

Seismicity

The seismological network of the Piton de la Fournaise Volcanological Observatory consists of 41 seismological stations currently in operation, representing a total of 109 channels sampled at 100 Hz and transmitted in real time to the observatory. This network includes 32 three-component broadband stations, 2 three-component short-period stations and 7 analogue stations with one vertical component. **Due to the eruption that started on February 13, 2026, two seismic stations (the PVD and GPS stations) threatened by lava flows had to be urgently dismantled by OVPF teams, with assistance from Section Aérienne de Gendarmerie and Peloton de Gendarmerie de Haute Montagne.**

Earthquakes are located based on the arrival times of P and S waves, which are manually plotted in the SeisComP software (www.seiscomp.de) using automatic or visual detections. The earthquakes are then located using NonLinLoc software (Lomax et al., 2000), using a three-dimensional velocity model. This model takes into account a velocity gradient according to the topography and assumes a constant VP/VS ratio of 1.7. The P-wave velocity is 3.3 km/s at the free surface and increases linearly with depth at a gradient of 0.3 s^{-1} .

Observations

In April 2026, the OVPF-IPGP recorded at Piton de La Fournaise:

- 1020 shallow volcano-tectonic earthquakes (0 to 2.5 km above sea level) below the *Bory* and *Dolomieu* summit craters;
- 64 deep volcano-tectonic earthquakes (below sea level);
- 45 long-period earthquakes;
- 607 rockfalls;
- as well as the recording of a tremor associated with the eruption that started on February 13, 2026, and stopped on April 12, 2026 (see section B for more details).

April was marked by **intense shallow seismic activity beneath the summit at the end of the two periods of renew of surface activity, namely on April 1 and 2 and April 11 and 12** (Figure 1). These earthquakes were mainly located at the roof of the shallow magma reservoir, between 0.3 and 1.2 m above sea level (Figure 2), and were linked to a destabilization of this roof caused by the depletion of the reservoir feeding the eruption.

Following the end of the eruption on April 12 (7:10 p.m. UTC):

- a **resumption of deep seismic activity** is recorded since April 13. These earthquakes, reflecting an upwelling of deep magma toward the shallow reservoir, were located between 6 and 7.2 km below sea level west of the Bory crater (Figure 2). To monitor seismic activity, an automatic “template matching” detection has been performed in near real time since 2016. Figure 3 shows the number of deep earthquakes detected and relocated since April 1, 2026.
- **numerous long-period earthquakes** were also recorded, mostly between April 13 and 21 (Figure 1), particularly during the post-eruptive tremor phases. This type of earthquake indicates fluid circulation at depth, confirming the presence of magma at shallow depth during the tremor phases recorded until April 21.



In addition, **607 rockfalls** were detected during the month, mainly inside the *Dolomieu* crater, along the cliffs of the *Enclos Fouqué* caldera and of the *Cassé de la Rivière de l'Est*, as well as on the recently formed cones and lava flows. This type of gravitational activity is common at Piton de la Fournaise, although it was more intense this month due to instability in the eruptive cones and recent lava flows.

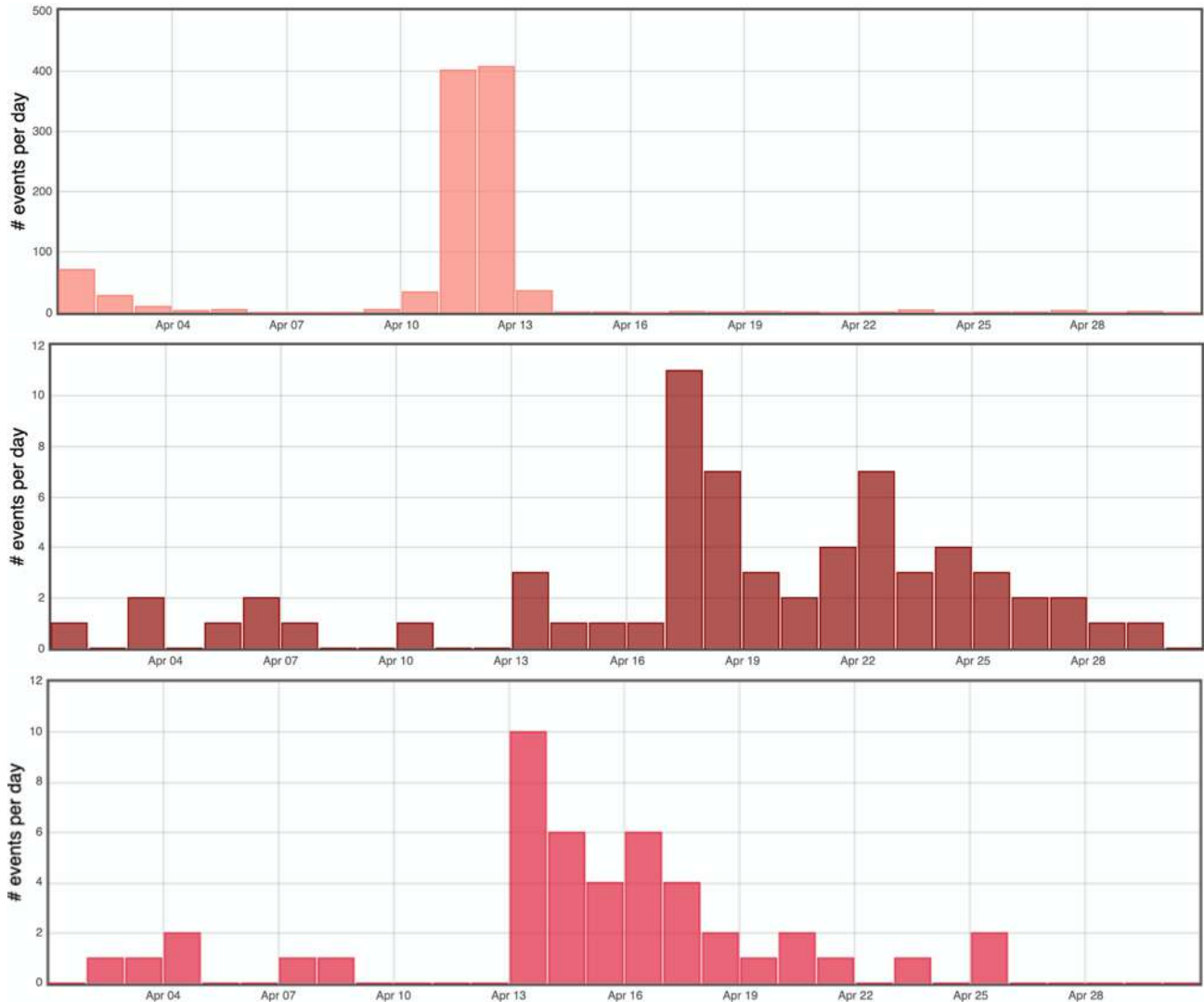


Figure 1: Number of (top) shallow volcano-tectonic, deep volcano-tectonic (middle) and long-period (bottom) earthquakes per day recorded in April 2026 (©WebObs/OVPF-IPGP).

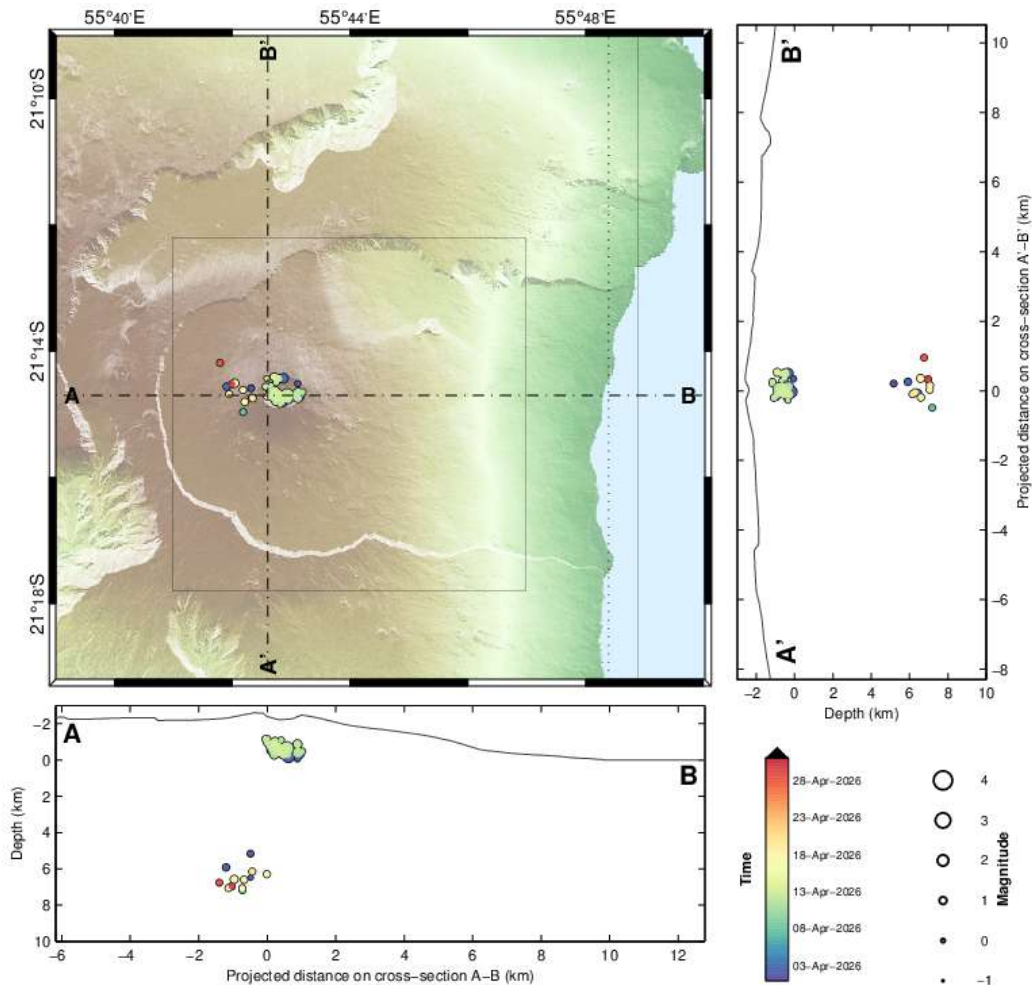


Figure 2: Seismicity below Piton de la Fournaise in April 2026. Location map (epicenters) and north-south and east-west cross-sections (hypocenters) of earthquakes as recorded by OVPF-IPGP. Only manually located earthquakes are shown on the map (©WebObs/OVPF-IPGP).

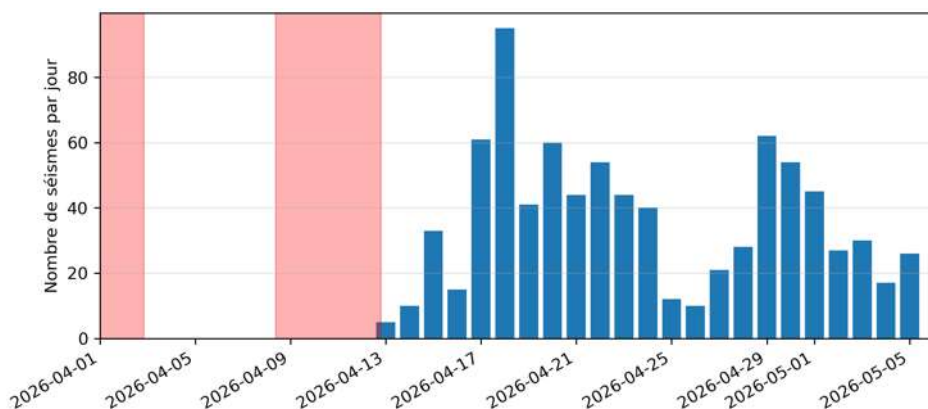


Figure 3: Number of earthquakes per day detected by template matching and relocated between April 1 and May 5, 2026. The eruptive periods are indicated in red (©OVPF-IPGP).



Deformation

The permanent network for monitoring deformation at Piton de la Fournaise currently comprises:

- 27 GNSS (Global Navigation Satellite System) stations,
- 11 pairs of tiltmeters at 10 different sites,
- 3 three-component extensometers.

Once the data have been retrieved (every 15 min to every day depending on the stations), they are automatically processed using the GipsyX/JPL software (Bertiger et al., 2020; Murphy et al., 2024).

These calculations incorporate the new JPL products in ITRF2020 (Altamimi et al., 2023, Rebischung et al., 2024). The calculated coordinates are expressed relative to the Figure Centre (FC), a concept more suited to small-scale area of work.

Observations

The ground deformation recorded in April 2026 were correlated with eruptive activity. Thus, the two phases of renewed activity, observed between March 28 and April 2 and between April 8 and 12, were preceded by inflation phases, with an elongation of approximately 7–8 mm of the summit baseline lines (Figures 4, 5 and 6). This inflation phase is linked to the re-pressurization of the shallow magma reservoir located between 1.5 and 2 km below the summit.

Conversely, during these two phases of renewed surface eruptive activity, deflation of the edifice was recorded, linked to the emptying of the reservoir (Figures 4, 5 and 6).

Following the end of the eruption on April 12, 2026, an inflation has been recorded once again.

Numerical modelling

Modeling of deformation sources for the period from April 12 to 30, 2026, shows the activation of two sources: one centered beneath the summit, corresponding to the re-pressurization of the shallow magma reservoir, and a deeper source offset to the west, likely indicating a resumption of magma supply to the magmatic system from a deeper source (Figure 7), as observed with the deep seismicity.

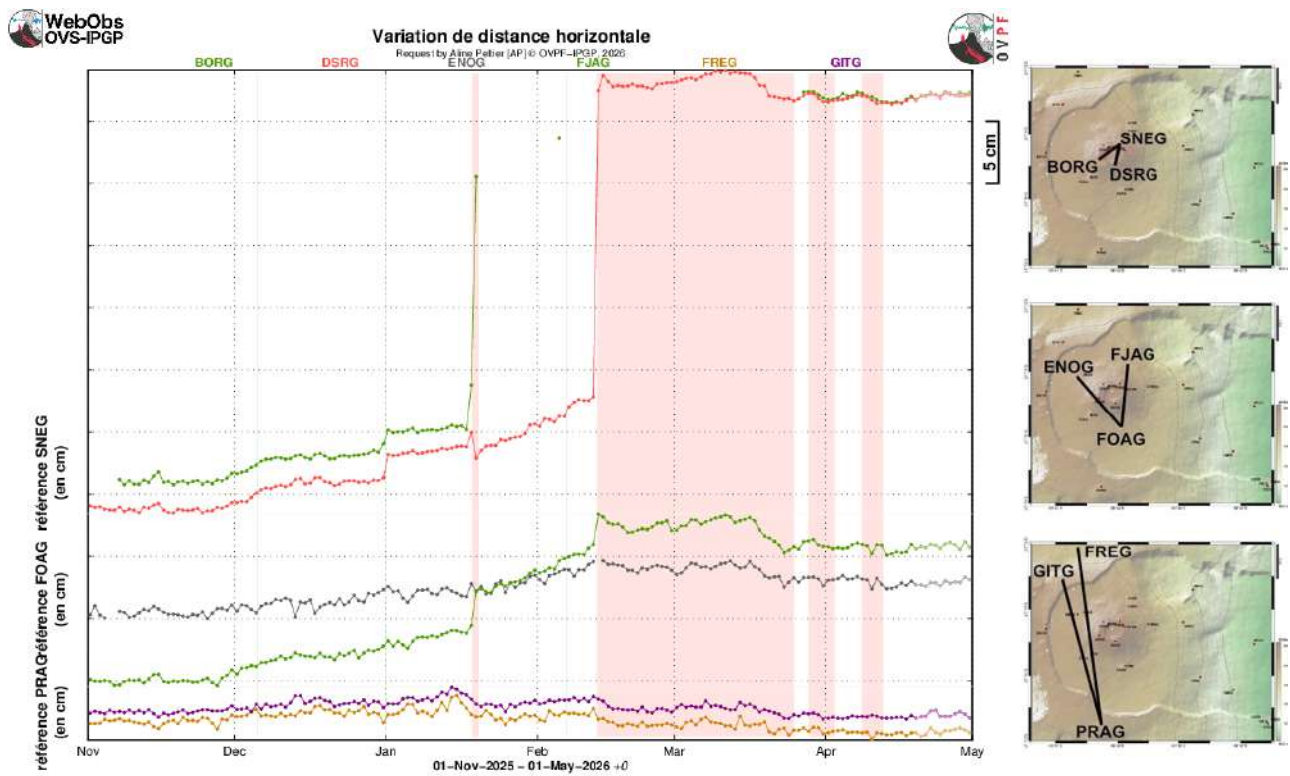


Figure 4: Ground deformation records over the past six months (the red and green bars represent eruptive and intrusive periods, respectively). The time series plots show the changes in horizontal distance between pairs of GNSS stations located around the Dolomieu summit crater (reference: SNEG; top graph), the terminal cone (reference: FOAG; middle graph) and the Enclos Fouqué caldera (reference: PRAG; bottom graph), from north to south (see location on the right). Increasing distances (or baseline elongation) indicate volcano inflation, while decreasing distances (or baseline contraction) reflect edifice deflation (©Webobs/OVPF-IPGP).

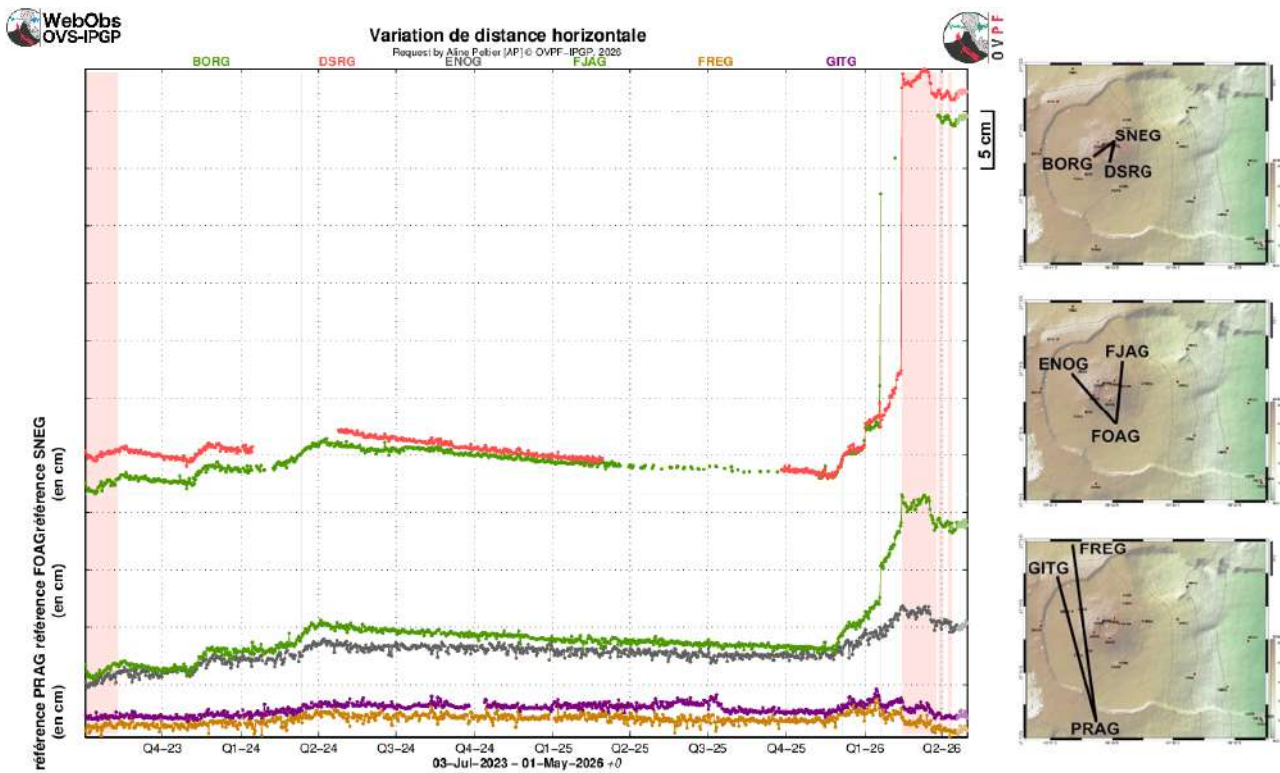


FIG0501 (X) BASILINEL - 03-Jul-2023 - 01-May-2026 (27 +0) - géo. (2023-04-07) WebObs MREXEV

Figure 5: Ground deformation records since the eruption of July-August 2023 (the red and green bars represent eruptive and intrusive periods, respectively). The time series plots show the changes in horizontal distance between pairs of GNSS stations located around the Dolomieu summit crater (reference: SNEG; top graph), the terminal cone (reference: FOAG; middle graph) and the Enclos Fouqué caldera (reference: PRAG; bottom graph), from north to south (see location on the right). Increasing distances (or baseline elongation) indicate volcano inflation, while decreasing distances (or baseline contraction) reflect edifice deflation (©WebObs/OVPF-IPGP).

* Glossary: The summit GNSS signals indicate the influence of a shallow pressure source below the volcano, while distant GNSS signals indicate the influence of a deep pressure source below the volcano. Inflation usually means pressurization; and conversely deflation usually means depressurization.

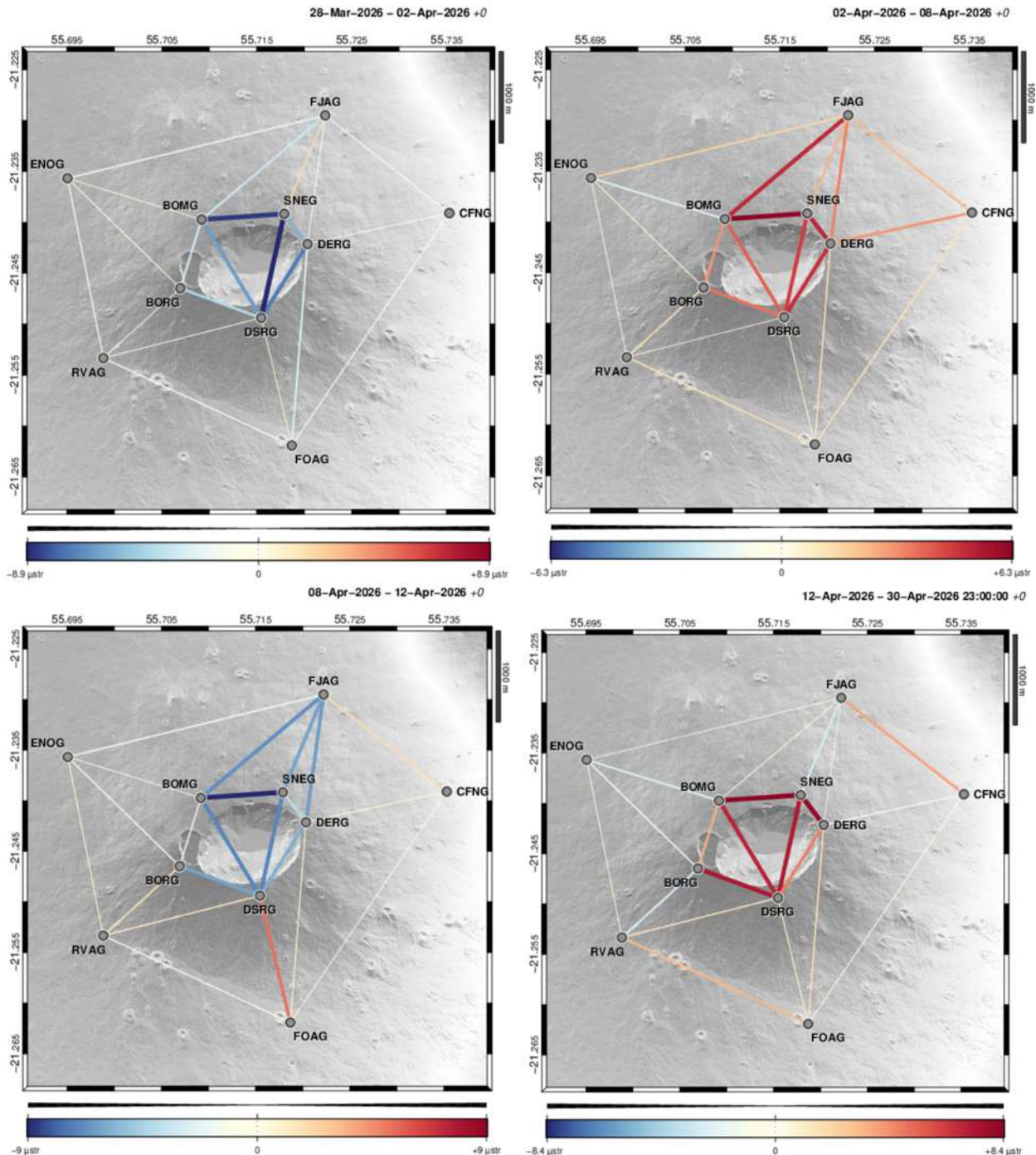


Figure 6: Linear 3-D strain maps (in μ strain, or a deformation of one millionth) for (left to right and up to bottom) the deflation period of March 28 to April 2, 2026, the inflation period of April 2 to 8, 2026, the deflation period of April 8 to 12, 2026, and the inflation period of April 12 to 30, 2026. The thickness and color of the baselines indicate the intensity of the strain, either compressive (in blue) or tensile (in red) (©WebObs/OVPF-IPGP, topography ©IGN LIDAR 2025).



GNSS GIPSYX Pdf OVPF - Source modelling
Request by Aline Peltier [AP] © OVPF-IPGP, 2026

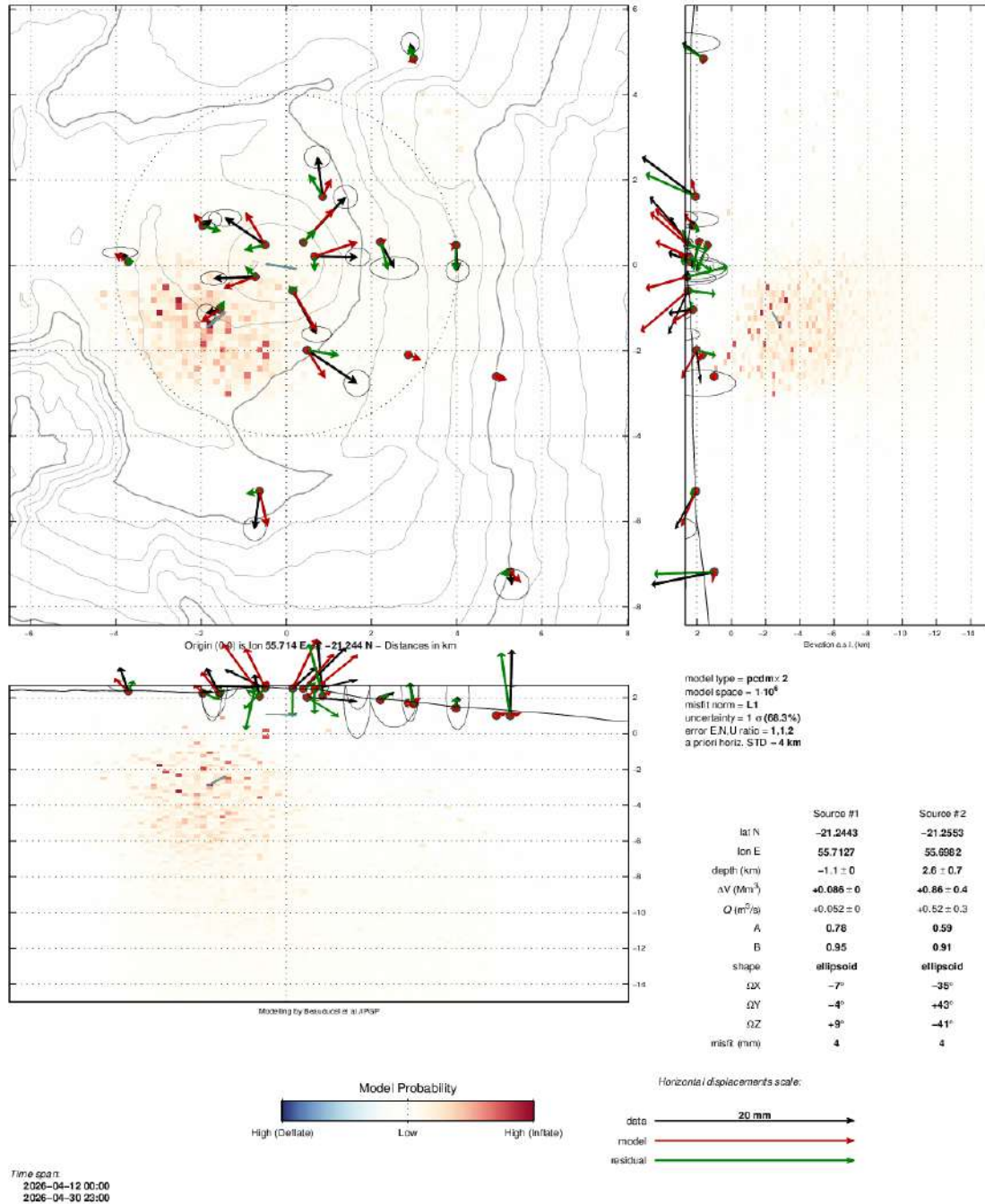


Figure 7: Modelling of the pressure sources responsible of ground displacements (pCDM models, Nikkhoo et al., 2016) linked to the inflation period of April 12 to 30, 2026. The black vectors represent observed data, the red vectors represent modelled vectors, and the green vectors represent the residuals between observed and modelled vectors. The characteristics of each source (primary #1 and secondary #2) are listed in the lower right corner (©Webobs/OVPF-IPGP).



Gas geochemistry

The permanent geochemical network for monitoring gas emissions from Piton de la Fournaise currently comprises:

- 3 MAX-DOAS stations measuring the optical thickness of SO₂ (ppm.m) in the atmosphere. Measurements are taken every 10 to 15 minutes during the day when weather conditions are favorable (Arellano et al., 2020).
- 1 MultiGaS station measuring excess H₂O, CO₂, SO₂ and H₂S relative to the atmosphere, with measurements taken every 6 hours.
- 4 stations measuring CO₂ flux through the soil. At these stations, meteorological parameters (temperature, pressure, humidity, wind speed and direction) are also recorded in order to correct signals from environmental disturbances (Boudoire, 2017; Bénard et al., 2023). Measurements are taken every hour.

CO₂ concentration in the soil

Since 2025, average CO₂ soil emissions tend to be constant on the most distal stations (BLEN, PNRN) and to increase on the most proximal stations (PCNR, GITN). That marks a clear evolution with respect to the long term of decrease recorded in the period 2021-2025 on these sites (Figure 8).

In 2026, the strongest increase in soil CO₂ emissions have been recorded during the February-April eruption on PCRN and GITN stations.

PCRN station shows a marked trend of decrease since the end of the February-April 2026 eruption.

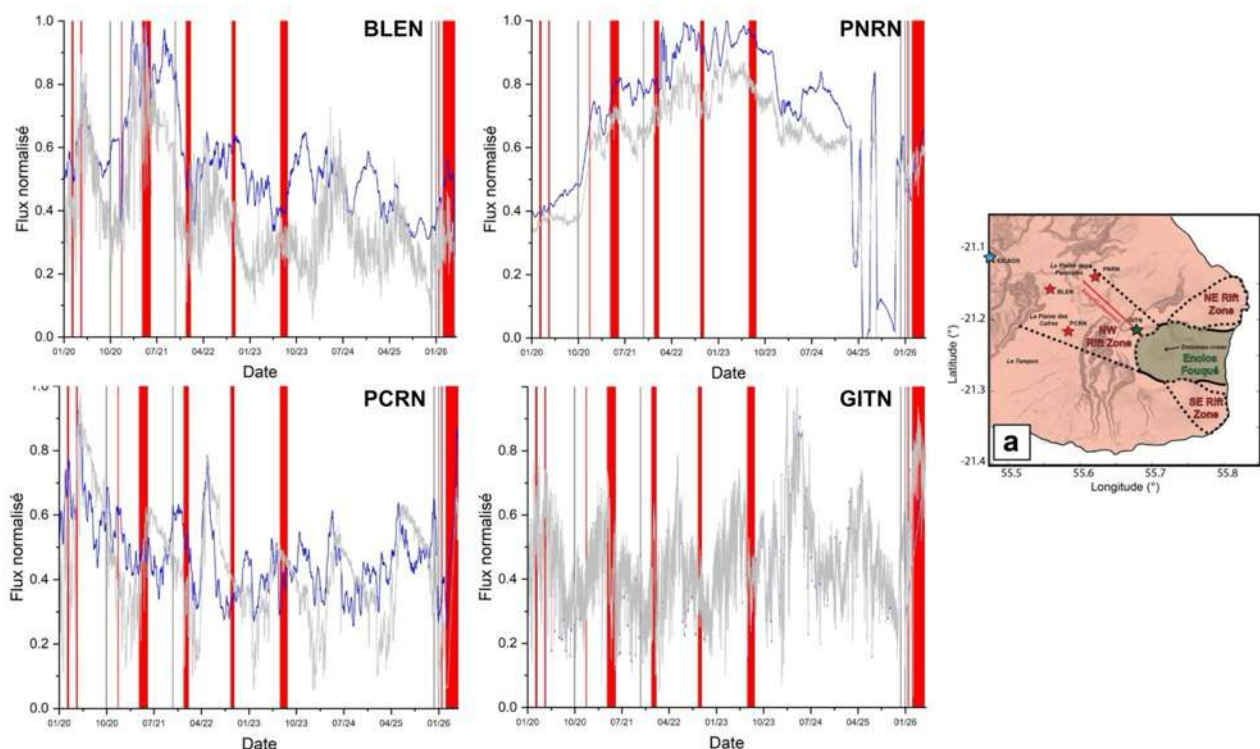


Figure 8: Normalized CO₂ soil emissions (grey: raw data) corrected for short period influence of environmental parameters (OVPF-correction model; 15 days moving average; in blue) of all CO₂ stations (see location on the map on the right). Red bars: eruptions; Gray bars: intrusions (©OVPF-IPGP-OSUL).



* Glossary: CO_2 is the first gas to be released from deep magma (rising from the mantle), so its detection in the far field often means a deep rise of magma. Its near-field evolution may be related to magmatic transfer in the shallowest part of the feeding system (< 2-4 km below the surface).

Summit fumaroles composition obtained by the MultiGas method

Since the end of the February – April 2026 eruption, only weak SO_2 and H_2S concentrations (< 0.1 ppmv) are recorded in the atmosphere at the volcano summit (Figure 9), typical of background values recorded during quiescence phases.

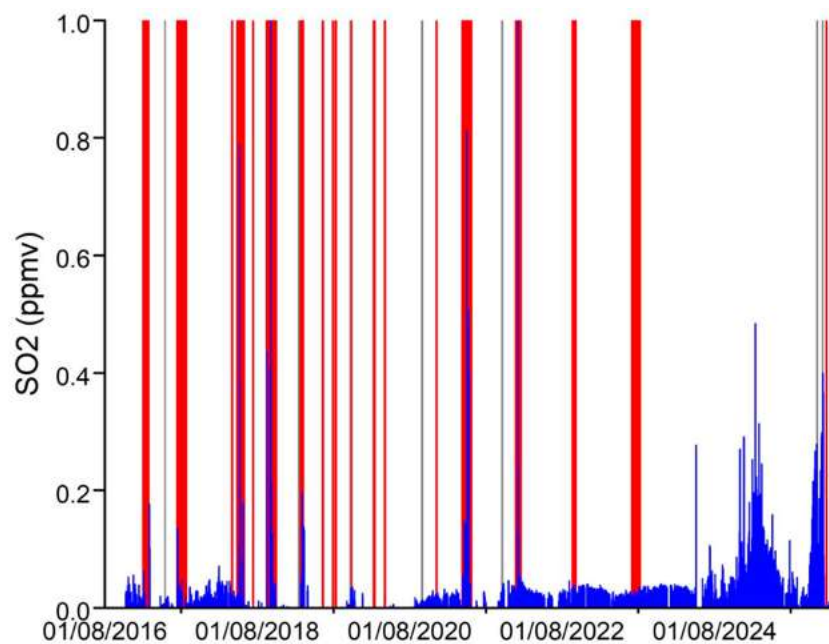


Figure 9: Raw (in blue) concentrations of SO_2 in the atmosphere at the summit of Piton de la Fournaise (MultiGas station) Red bars: eruptions; Gray bars: intrusions (©OVPF-IPGP-OSUL).

* Glossary: The MultiGas method allows measuring the concentrations of H_2O , H_2S , SO_2 and CO_2 in the atmosphere at the summit of the Piton de la Fournaise volcano. Magmatic transfer in the Piton de la Fournaise feeding system can result in an increase in SO_2 concentrations and in the C/S ratio (carbon/sulfur).

SO_2 flux in the air obtained by DOAS method

The NOVAC stations located on the edges of the Enclos Fouqué (“Enclos0” to the west, “Piton de Bert” to the south, and “Piton Partage” to the north) detected the gas plume associated with the eruption of February 13 – April 12, 2026.

The start of the February 2026 eruption was associated with a very high SO_2 flux (up to >10 kton/day on February 13). These emissions decreased rapidly between February 13 and 15, before to increase (up to > 5 kton/day) again on March 16, March 20-23, March 30 and April 11. These SO_2 fluxes are shown in section B of this bulletin (Figure 21).



* Glossary: During rest periods, SO₂ flux at Piton de la Fournaise is below the detection threshold. The SO₂ flux may increase during magma transfer in the shallowest part of the feeding system. During eruptions, it is directly proportional to the amount of lava emitted at the surface.

Phenomenology

April 2026 was marked by the **end of the eruption that began on February 13, 2026. The eruption ended on April 12 (7:10 p.m. UTC).**

This eruption was characterized by two pauses in activity:

- . between March 25 (12:30 p.m. UTC) and March 28 (11:00 a.m. UTC)
- . and between April 2 (8:10 p.m. UTC) and April 8 (9:15 a.m. UTC) (see Section B for more details).

Three phases of tremor without eruptive activity were also recorded during the second pause and following the end of the eruption:

- . from April 3 (4:40 p.m. UTC) to April 8 (9:15 a.m. UTC),
- . from April 14 (11:00 a.m. UTC) to April 15 (7:20 a.m. UTC),
- . and from April 19 (2:20 a.m. UTC) to April 21 (12:10 p.m. UTC).

Summary

The eruption that started on February 13, 2026, ended on April 12 2026. A detailed summary is provided below in section B of this bulletin. The onset of the eruption and related observations were described in the February and March 2026 monthly bulletins.



B. The February 13 – April 12, 2026 eruption

* Information regarding the onset of this eruption can be found in the OVPF-IPGP monthly bulletins for February and March 2026.

* Detailed day-by-day information can be found in the OVPF-IPGP's special daily bulletins, available at this link: <https://www.ipgp.fr/communiqués-et-bulletins-de-l'observatoire/?categorie=&domaine=&date=&observatoire-associe=391&motcle=>

Surface activity

Following the opening of four eruptive fissures on February 13 along the eastern and southeastern outer edges of the *Dolomieu* crater and on the volcano's east-southeastern flank, activity has been concentrated at a single eruptive site since February 14. This site is located on the lowest fissure, which opened on the east-southeast flank at an elevation of 2,056 meters.

The concentration of activity at a single site allowed for the formation of an eruptive cone created by the accumulation of lava projections and overflows, and the lava flows have gradually advanced toward the eastern flank of the volcano, with the development of lava tubes (flows confined beneath a solidified crust) that has allowed the lava to be isolated from the atmosphere and to resurface further downstream at numerous breakouts.

The lava field, extending downstream from the volcanic cone, has formed two main branches (the northern and southern branches, Figure 10).

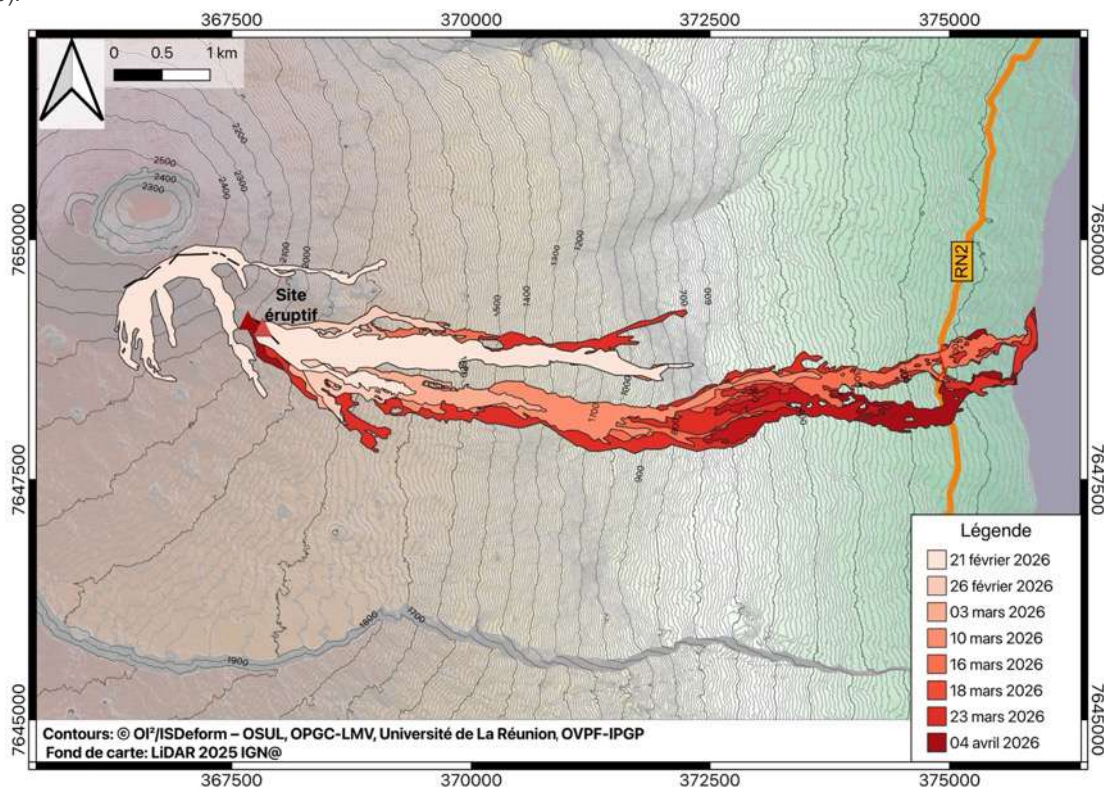


Figure 10: Map of lava flows associated with the February 13 – April 12, 2026, eruption at Piton de la Fournaise. The colored areas indicate the boundaries of lava flows on various dates listed in the legend. These boundaries were determined by analyzing satellite imagery. (© OI²/ISDeform – OSUL, OPGC-LMV, Université de La Réunion, OVPF-IPGP).



One month after the eruption started, **on March 13 at 8:02 a.m. (local time), the southern branch's lava flow reached National Route 2**, located more than 7 kilometers from the eruptive site (see OVPF daily bulletins for more details). Three days later, in the early hours of March 16 around 12:20 a.m., it finally reached the ocean, having traveled approximately 825 meters below the road (Figures 10 and 11).

At the point where the lava met the ocean, a platform formed as a result of the accumulation of lava flows and fine particles from the fragmentation of the lava, as well as a plume of acidic gas, called "laze" (lava haze), consisting of water vapor, hydrochloric acid (HCl), and fine particles.

Following the first lull in the eruption on March 28 and the resumption of activity between March 28 and April 2 and between April 8 and 12, the lava platform did not grow (no lava flow was detected there after March 30, Figure 11); however, National Route 2 was again cut off by lava on April 1 and 2 (Figures 12, 13, and 14), approximately 300 m further south than the previous cutoff point (Figures 10 and 15).

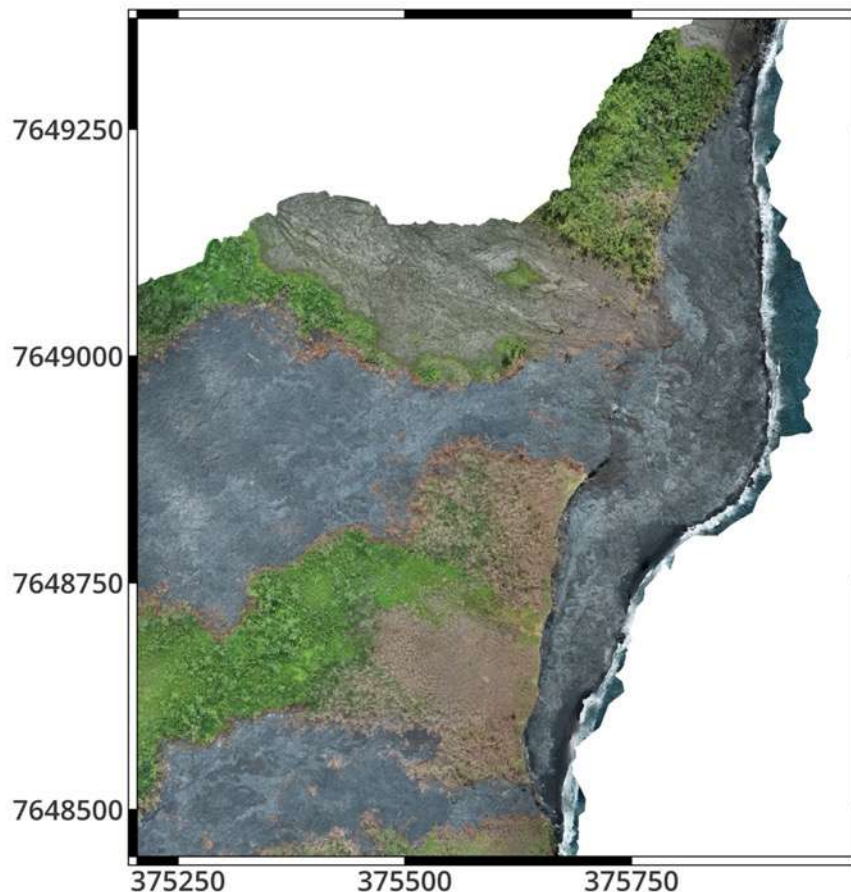


Figure 11 : Photo of the platform taken on April 9, 2026 (©Université de la Réunion-OVPF-IPGP).



Figure 12: Photo of the lava reaching the national road on April 1st, 2026 at 21h29 local time (©Gendarmerie).



Figure 13: Photos of the lava reaching the national road on April 2nd, 2026. Photos taken (to the left) at 8h15 (to the right) at 9h12 local time (©OVPF-IPGP).



Figure 14: Photo of the lava reaching the national road on April 2nd, 2026 at 13h01 local time (©OVPF-IPGP).

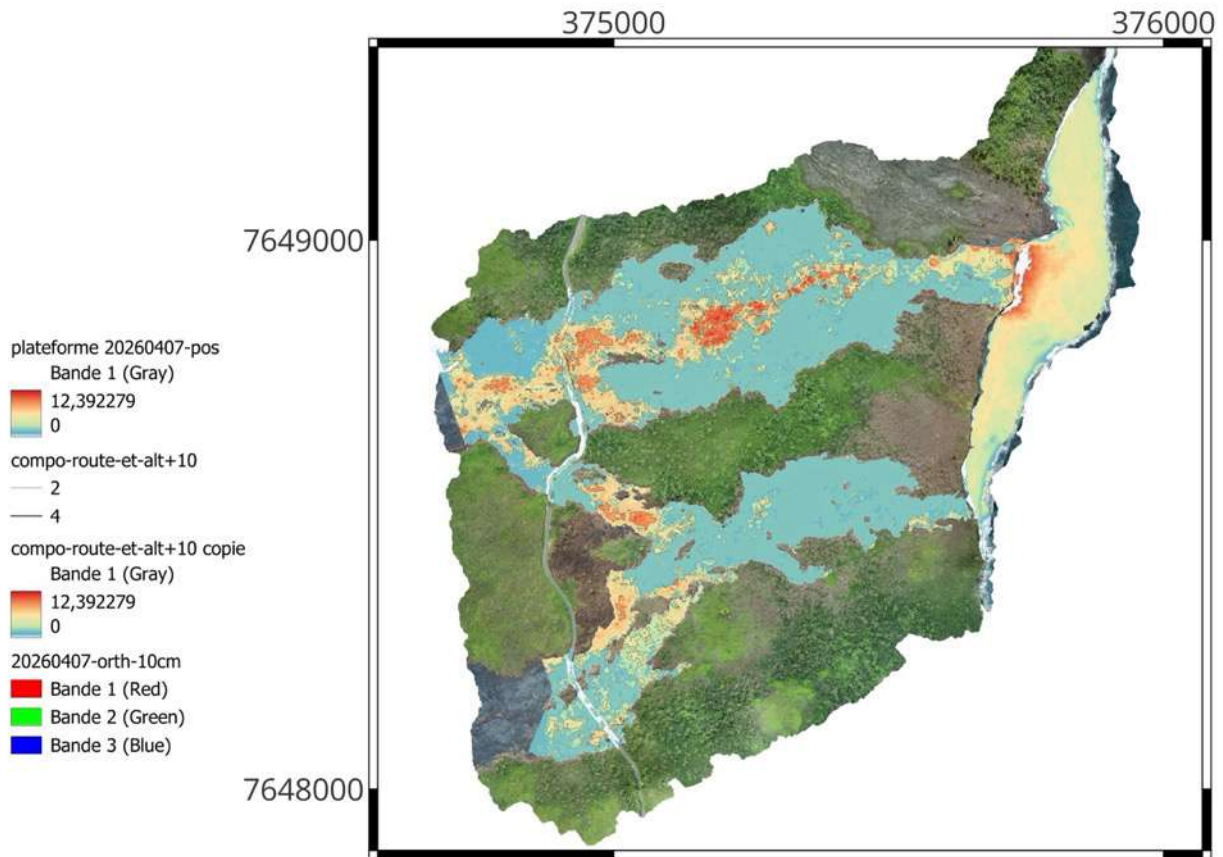
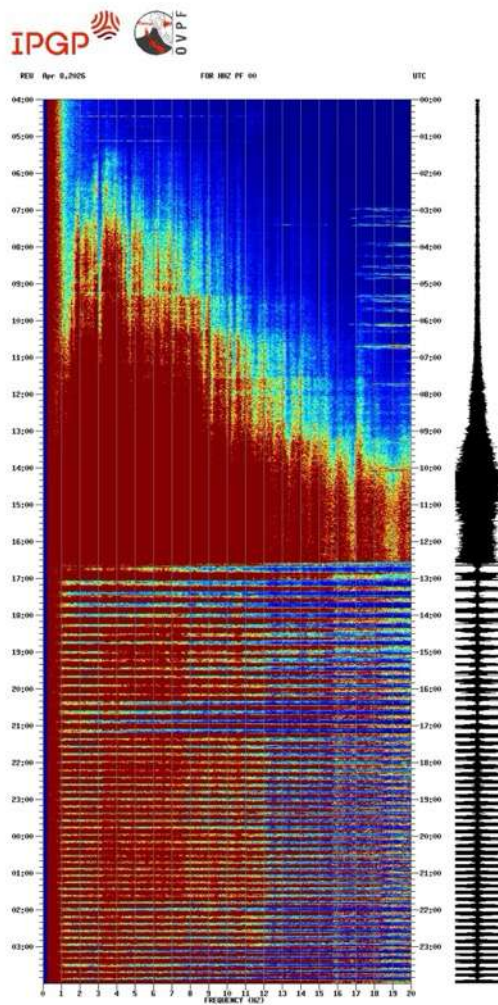


Figure 15: Map of lava flow thicknesses along and upstream of National Route 2, based on drone imagery analysis (©University of Réunion-OVVF-IPGP).

During the third phase of activity, which began on April 8 (9:15 a.m. UTC, 1:15 p.m. local time), intermittent activity was observed at the eruptive cone, accompanied by intermittent tremor phases (known as “piston gas” tremors). These phases correspond to activity involving intense projections and degassing for about 10 minutes, followed by lulls lasting about 10 minutes as well (Figures 16 and 17).

This phase of intermittent activity led to the opening of a new vent, approximately 180 m upstream of the eruptive cone formed since February 13 (Figure 18). The opening of this new vent marked the end of intermittent activity at the eruptive cone formed since February 13, where a lava lake and low activity persisted until the end of the eruption. It should be noted that no new dikes formed or propagated in connection with this new vent. This new vent is thus linked to the same dike as the one opened on February 13.

Activity then concentrated mainly on this new vent, allowing a new cone to form (Figure 18).



Phases de reprise de trémor
Phases d'arrêt de trémor

Figure 16: Spectrogram from the FOR seismic station located near the eruption site on April 8, showing the periods when tremor and eruptive activity (visible in the photos) ceased and resumed (©OVPF-IPGP).

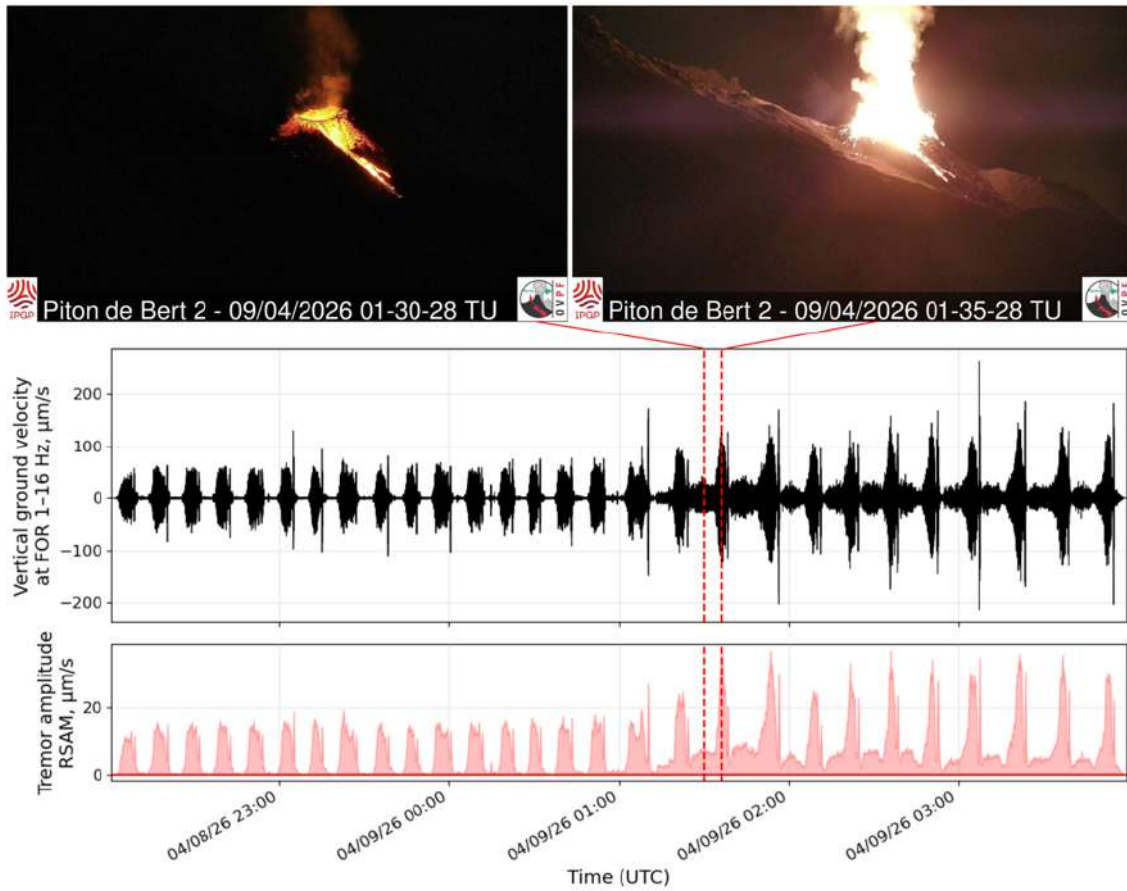


Figure 17: Comparison of surface observations from the BERT camera (top), seismic records (middle), and RSAM amplitude of the tremor (bottom) during the intermittent activity phase from April 8 to 9, 2026. (©OVPF-IPGP).



Figure 18: Photos of the eruptive cones on April 9 and 12, 2026, from the Piton de Bert webcam (©OVPF-IPGP).



Lava flow rates

Lava flow rates, estimated from satellite data using the HOTVOLC (OPGC – Clermont Auvergne University) and MIROVA (University of Turin) platforms, reached values as high as $63 \text{ m}^3/\text{s}$ during the first hours of the eruption, then declined as activity on the first fissures ceased (Figure 19). Between February 16 and March 18, average lava flow rates were $< 20 \text{ m}^3/\text{sec}$ and, most of the time, ranged between 1 and $10 \text{ m}^3/\text{sec}$ (Figure 19).

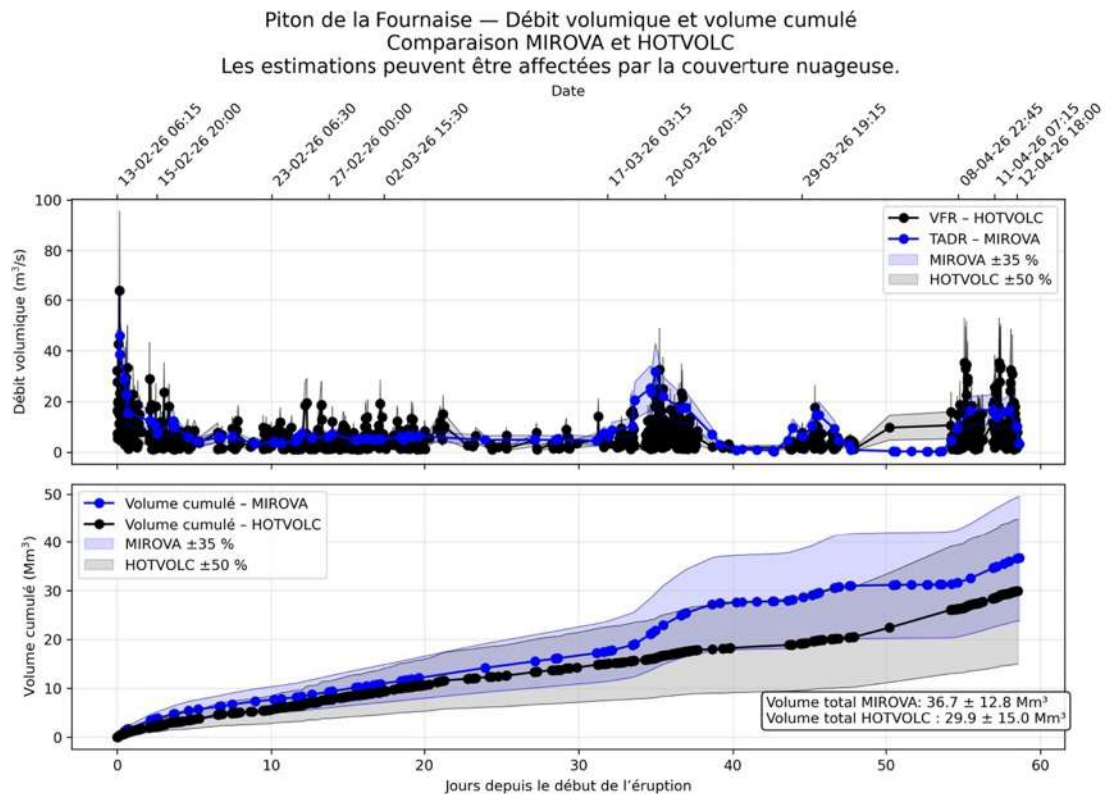


Figure 19: Estimates of surface lava flow rates (m^3/s) and the cumulative volume of lava emitted at the surface (millions of m^3 , Mm^3) based on satellite data from the HOTVOLC (in black, ©OPGC-Clermont Auvergne University) and MIROVA (in blue, ©University of Turin) platforms between February 13 and April 12, 2026.

An increase in flow rates was recorded between March 17–18 and March 20 (peaking at $25 \text{ m}^3/\text{sec}$). This increase occurred during the most intense deflation phase in the summit area (a deflation phase that lasted until March 23, Figure 19) and during the increase in shallow volcano-tectonic seismicity (located beneath the summit, Figure 20) that lasted from March 18 to 22.

This deflation phase, accompanied by increased shallow seismicity and higher flow rates, was interpreted as **a phase of depressurization of the shallow magma reservoir, accompanied by a mechanical response of the edifice and an increase in surface eruptive activity**. Note that there is a slight lag between the increase in tremor and the increase in flow rates, which may be due to uncertainties in lava flow rate measurements. Indeed, lava flow rate estimates derived from satellite methods may be underestimated due to observational biases, particularly those related to weather conditions (cloud cover), the development of flow within lava tubes, and the flow's entry into the sea, which limit the detection of thermal radiation.

The increase in lava flow rates was correlated with a rise in SO_2 fluxes measured by satellite (TROPOMI) and by the OVPF's NOVAC network (Figure 21).

As deflation slowed down until the eruption stopped on March 25, a gradual decrease in lava flow rates was observed, along with a decrease in summit seismicity (Figure 20).



The two periods of pause in the eruptive activity, from March 25 to 28 and from April 2 to 8, were marked by a resumption of edifice inflation and an increase in deep seismicity between 8 and 10 km below the western part of the summit (Figure 20). These observations suggest new inflows of deep magma into the shallow reservoir, leading to a re-pressurization of the magmatic system prior to the resumption of the eruption.

During the two phases of renewed activity, from March 28 to April 2 and from April 8 to April 12, deflation of the edifice linked to the emptying of the reservoir was observed, in a dynamic comparable to that observed between March 18 and 25 (Figure 20). The tremor peaks were correlated with peaks in surface lava flow rates and SO₂ fluxes into the atmosphere (Figures 20 and 21)

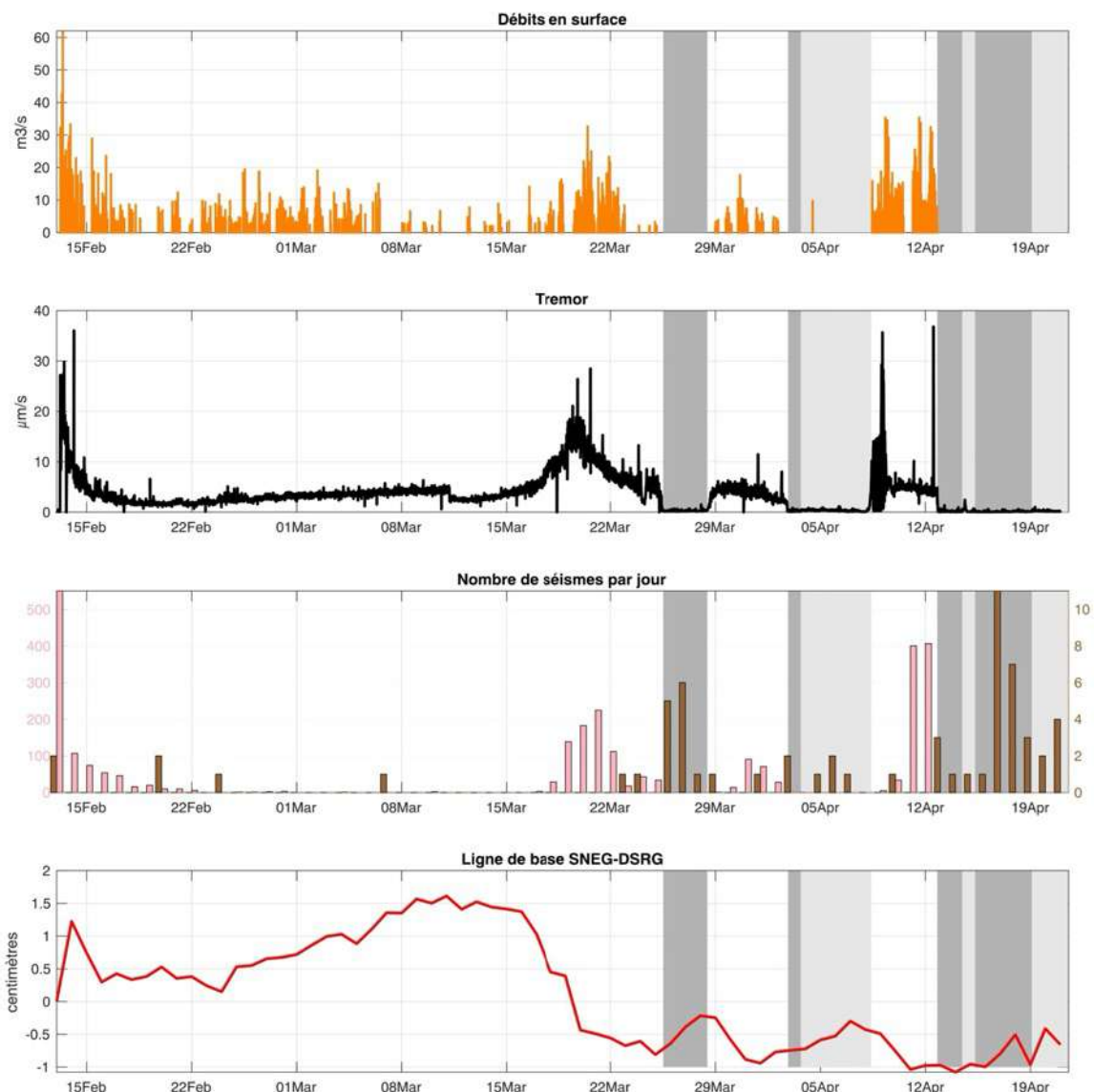


Figure 20: Summary of observations during the February 13 - April 12, 2026 eruption and the subsequent periods of tremor. Surface lava flow rates estimated by Hotvolc (in m³/s, ©OPGC-Clermont Auvergne University), volcanic tremor intensity (in µm/s, ©OVPF-IPGP), the number of shallow (in pink) and deep (in brown) volcano-tectonic earthquakes per day (©OVPF-IPGP), and the evolution of the SNEG-DSRG summit baseline (in cm) between February 13 and April 21, 2026. The periods without surface activity are shown in gray, the ones with tremor in light gray (©OVPF-IPGP).



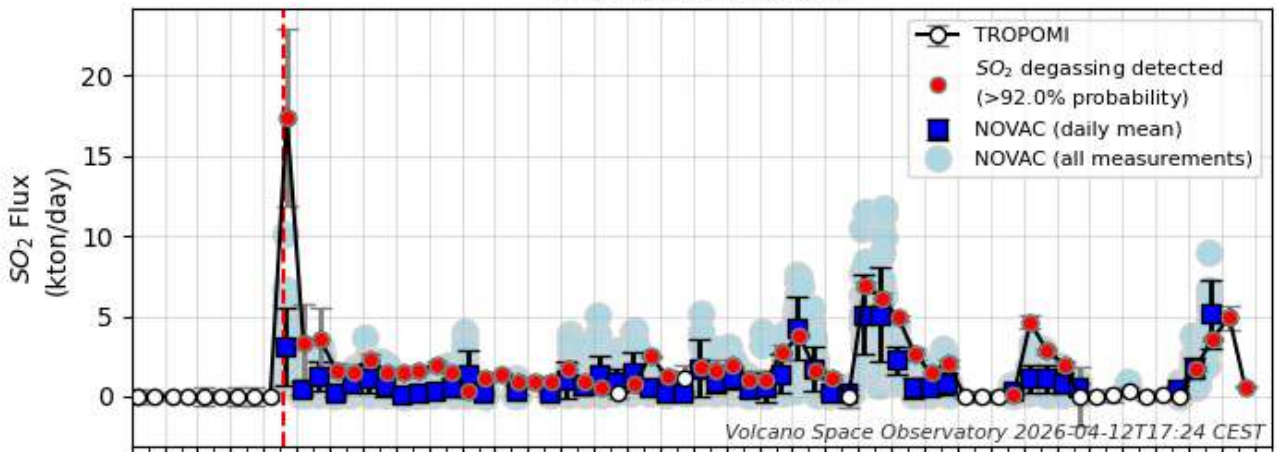
Piton de la Fournaise

Analysis: Volcano Space Observatory © ICARE/AERIS/FormaTerre/LOA/IPGP

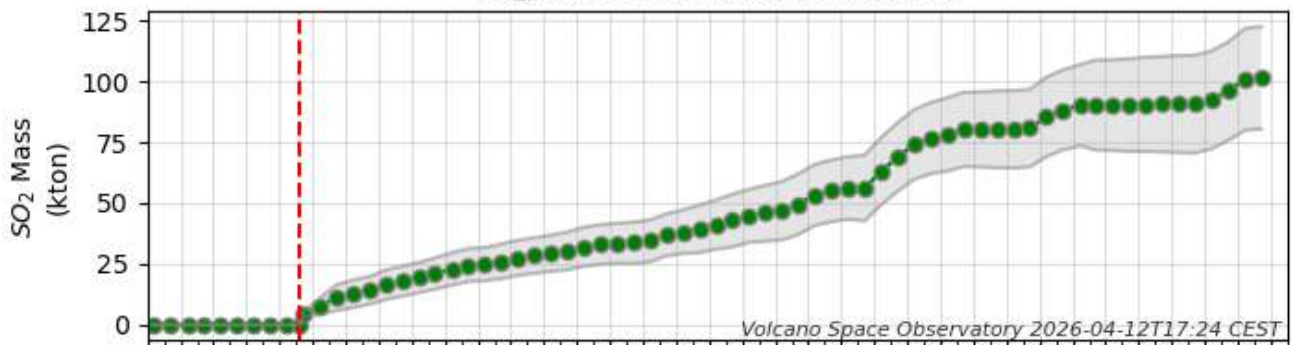
Satellite data: TROPOMI/Sentinel-5P © ESA/Copernicus

Ground-based data: NOVAC © OVPF/IPGP/Chalmers Univ

SO₂ Flux versus time



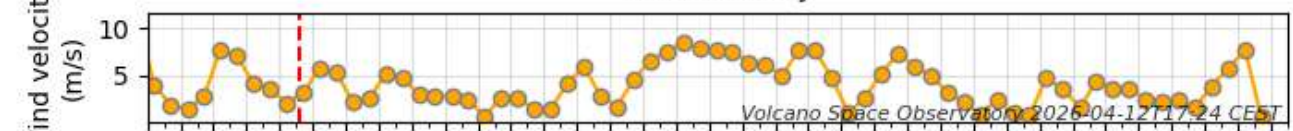
SO₂ Cumulative mass versus time



Mean cloud fraction within 50 km



Wind velocity



04 06 08 10 12 14 16 18 20 22 24 26 28 02 04 06 08 10 12 14 16 18 20 22 24 26 28 30 Apr 03 05 07 09 11 13
2026-Apr

Figure 21: Trends in sulfur dioxide (SO₂) flux measured by satellite (TROPOMI) and estimated by the NOVAC DOAS network. Top: daily SO₂ flux. Center: cumulative mass of SO₂ emitted. Bottom: average cloud cover within a 50-km radius. The vertical red line indicates the start of the eruption on February 13, 2026, at Piton de la Fournaise. (© Volcano Space Observatory; ICARE/AERIS/FormaTerre/LOA/IPGP; TROPOMI/Sentinel-5P – ESA Copernicus; NOVAC – Chalmers University of Technology – OVPF-IPGP).



Volume and duration of the eruption

The total volume of lava emitted at the surface, estimated based on surface lava flow rates (Figure 19), ranges between **29.9 (± 15) et 36.7 (± 12.8) million m^3** , and the surface of the **platform**, estimated using stereophotogrammetry, is approximately **8.5 hectares**. It should be noted that the unstable platform is showing signs of erosion at the point where it meets the ocean due to the action of the waves (Figure 22); its surface area will therefore decrease over time.

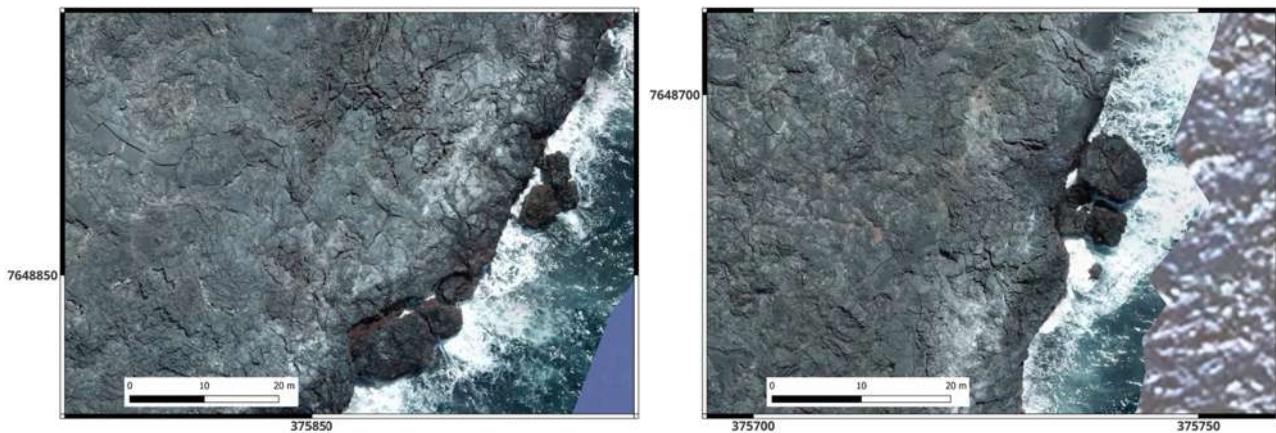


Figure 22 : Photos of the platform on April 7, 2026 (©Université de la Réunion-OVPF-IPGP).

The duration of this eruption, **50,1 days of eruptive activity** (compared to an average of 20 days for recent eruptions of Piton de la Fournaise), **can be explained by pressurization of the shallow magma reservoir** between February 24 and March 15 and during the two pauses, detected by the inflation of the volcano during these periods (Figure 20). **This pressurization is believed to be linked to the arrival of magma from deeper levels, thereby feeding the eruption.**

Preliminary results of the lava analysis

The initial magma from the January 18–20, 2026, eruption was a degassed magma, fairly dense (with a maximum pyroclastic density of 70%) and relatively “evolved” chemically (low magnesium content), poor in crystals, and exhibiting a glass transition temperature consistent with the magmas emitted at the end of the July–August 2023 eruption. These characteristics suggest that **the eruptive cycle, initiated by the January 2026 eruption, began by mobilizing a magma pocket derived from previous eruptions.**

At the start of the February 2026 eruption, the magma became hotter, and the explosions at the eruptive vents produced golden pumice that was extremely vesicular (over 90% vesiculation), a sign of the arrival of a more gas-rich magma. A clear segregation is then observed within the shallow dike during the eruption, with gas-rich pumice at the eruptive vents, and gas-poor lavas (average vesiculation of about 30–40%), including pahoehoe-type lavas, which formed locally to a greater extent due to topographic variations or yield strength.

In terms of overall rock composition, **an increase in magnesium content is observed during the February–April 2026 eruption, due in part to the incorporation of olivine crystals.**

At the midpoint of the eruption (March 15–16, 2026), the proportion of new magma remained low (10–15%) based on Sr isotopic compositions. In other words, >85 to 90% of the magma emitted up to March 16 was residual magma, likely reheated and remobilized by a deep injection.

The first signs of new magma at the surface appear after March 12; however, isotopic variations remain very small and at the limit of analytical error.

** As these results are preliminary, a more detailed analysis will be presented in one of the upcoming monthly bulletins.*



C. Seismic activity on La Réunion and in the Indian Ocean basin

Local and regional seismicity

In April 2026, the OVPF-IPGP recorded:

- 64 local earthquakes (below the island, within a radius of 200 km around the island, Figures 23 and 24);
- 3 regional earthquakes (in the Indian Ocean basin).

In April 2026, the OVPF-IPGP detected **64 local earthquakes**. 16 events were located, mostly beneath *La Roche Écrite*, *La Plaine des Palmiste*, *La Plaine des Cafres* and east of *Salazie* (Figure 23). Most of these earthquakes have **magnitude less than 1** and are difficult to locate accurately. These earthquakes were located between **10 km and 25 km depth in oceanic lithosphere** on which was built the volcanic edifice at the origin of La Réunion island.

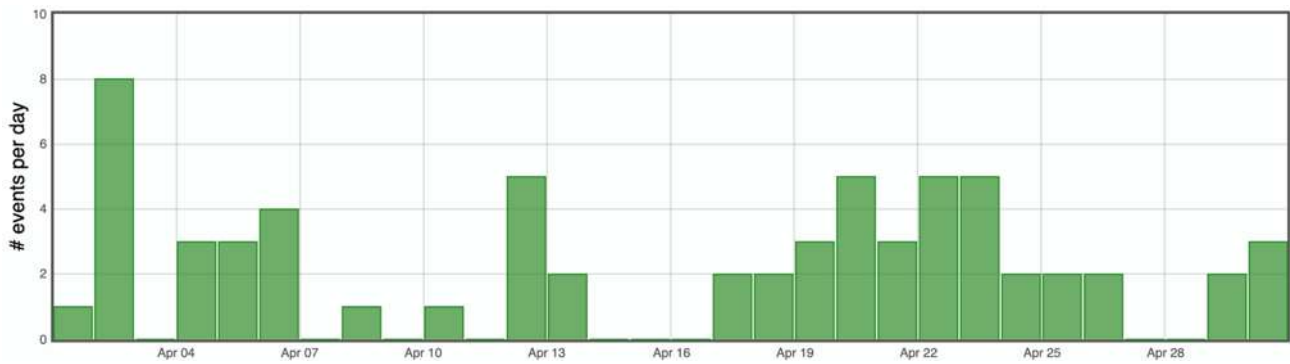


Figure 23: Number of local earthquakes (La Réunion island) per day recorded in April 2026 (©WebObs/OVPF-IPGP).

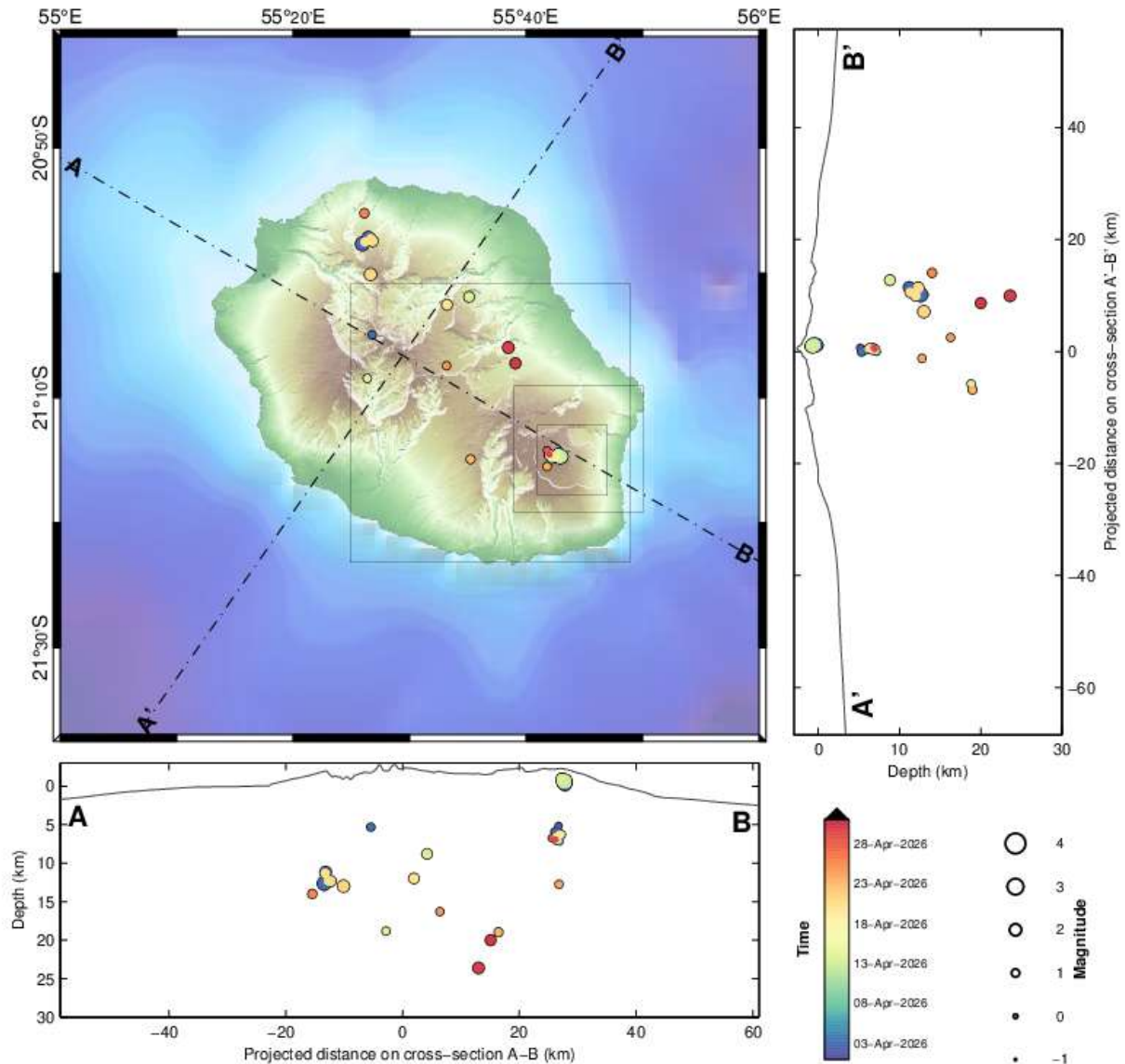


Figure 24: Seismicity below La Réunion in April 2026. Location map (epicenters) and north-west – south-east and south-west – north-east cross-sections (hypocenters) of earthquakes as recorded by OVPF-IPGP. Only localizable earthquakes are shown on the map (©WebObs/OVPF-IPGP).



Seismic-volcano activity in Mayotte

The « REseau de surveillance VOlcanologique et SIsfmologique de MAyotte (REVOSIMA) » is the structure in charge of the volcano and seismic monitoring of Mayotte. IPGP and BRGM coordinate and manage REVOSIMA. Operational monitoring of seismic-volcanic activity is carried out by IPGP (OVPF), under the joint responsibility of BRGM and in close association with IFREMER and CNRS. REVOSIMA is supported by a scientific and technical partnership. The REVOSIMA consortium: IPGP and Université Paris Cité, BRGM, IFREMER, CNRS, BCSF-RéNaSS, ITES and Université de Strasbourg, IGN, ENS, SHOM, TAAF, CNES, Université Grenoble Alpes and ISTerre, Université Clermont Auvergne, LMV and OPGC, Université de La Réunion, Université Paul Sabatier, Toulouse and GET-OMP, Université de la Rochelle, Université de Bretagne Occidentale, IRD and collaborators.

All information on the REVOSIMA and the activity in Mayotte can be found on the dedicated webpages:

- <https://www.ipgp.fr/observation/infrastructures-nationales-hebergees/revosima/>
- <https://www.ipgp.fr/actualites-du-revosima/>
- <https://www.facebook.com/ReseauVolcanoSismoMayotte/>
- <https://bsky.app/profile/revosima.bsky.social>

May 7, 2026
OVPF-IPGP Director



D. Appendix

Definition of Volcanic Alert Levels for Piton de la Fournaise

from *disposition spécifique « Volcan Piton de la Fournaise » - arrêté n°2242*- Emergency plan set up by the department responsible for the protection of the population in the event of unrest or activity of the Piton de la Fournaise

• **“Vigilance”**: possible eruption in medium term (a few days or weeks) or presence of risks on the sector (rockfalls, increase of gas emissions, still hot lava flows...).

Access to the Enclos Fouqué caldera and to the summit volcano are allowed with restrictions.

• **“Alert 1”**: probable or imminent eruption.

Access to the Enclos Fouqué caldera and to the summit are closed and prohibited.

• **“Alert 2”**: ongoing eruption.

Alert 2-1: ongoing eruption inside the Enclos Fouqué caldera without threat to the safety of people, property or the environment

Alert 2-2: ongoing eruption inside the Enclos Fouqué caldera with direct or indirect threat to the safety of people, property or the environment.

Access to the Enclos Fouqué caldera and to the summit are closed and prohibited. For Alert 2-2, evacuation of the people and vehicles depending on the issues.

• **“Alert 2-3”**: ongoing eruption outside the Enclos Fouqué caldera with threat to the safety of people, property or the environment.

Access to the Enclos Fouqué caldera and to the summit are closed and prohibited. Evacuation of the people and vehicles depending on the issues.

• **“Sauvegarde”**: end of eruption.

Evaluation of a partial reopening of the Enclos Fouqué caldera access.



References

- Altamimi, Z., Rebischung, P., Collilieux, X., Métivier, L., & Chanard, K. (2023), ITRF2020: an augmented reference frame refining the modeling of nonlinear station motions, *Journal of Geodesy*, 97(5), 47. <https://link.springer.com/article/10.1007/s00190-023-01738-w>
- Arellano, S., Galle, B., Apaza, F., Avard, G., Barrington, C., Bobrowski, N., ... Yalire, M. (2020), Synoptic analysis of a decade of daily measurements of SO₂ emission in the troposphere from volcanoes of the global ground-based Network for Observation of Volcanic and Atmospheric Change, *Earth System Science Data Discussions*, 2020, 1-3
- Beauducel, F., Roult, G., Ferrazzini, V., Peltier, A., Jousset, P., Boissier, P., Villeneuve, N. (2025), Jerk, a promising tool for early warning of volcanic eruptions. *Nat Commun* 16, 11418, <https://doi.org/10.1038/s41467-025-66256-z>
- Bénard, B., Di Muro, A., Liuzzo, M., Gurrieri, S., Boissier, P., Brunet, C. et al. (2023), Seasonal environmental controls on soil CO₂ dynamics at a high CO₂ flux sites (Piton de la Fournaise and Mayotte volcanoes), *Journal of Geophysical Research: Biogeosciences*, 128(6), e2023JG007409
- Bertiger, W., Bar-Sever, Y., Dorsey, A., Haines, B., Harvey, N., Hemberger, D., ... & Willis, P. (2020), GipsyX/RTGx, a new tool set for space geodetic operations and research, *Advances in space research*, 66(3), 469-489
- Bouidoire, G. (2017), Architecture et dynamique des systèmes magmatiques associés aux volcans basaltiques : exemple du Piton de la Fournaise. *Volcanologie*, Université de la Réunion, 2017. Français. (NNT : 2017LARE0022). (tel-01902958)
- Chevrel, MO., Labroquere, J., Harris, AJL, Rowland, SK (2018), PyFLOWGO: An Open-Source Platform for Simulation of Channelized Lava Thermo-Rheological Properties. *Comput. Geosci.* 111: 167–80. <https://doi.org/10.1016/j.cageo.2017.11.009>
- Duputel, Z., Lengliné, O., Ferrazzini, V. (2019), Constraining Spatiotemporal Characteristics of Magma Migration at Piton De La Fournaise Volcano From Pre-eruptive Seismicity, *Geophys. Res. Lett.* 46: 119-127, <https://doi.org/10.1029/2018GL080895>
- Favalli, M., Pareschi, MT., Neri, A., Isola, I. (2005), Forecasting Lava Flow Paths by a Stochastic Approach, *Geophys. Res. Lett.* 32(3): 1–4. <https://doi.org/10.1029/2004GL021718>
- Harris, AJL., Chevrel, MO., Coppola, D., Ramsey, MS., Hrysiwicz, A., Thivet, S., Villeneuve, N. et al. (2019), Validation of an Integrated Satellite-data-driven Response to an Effusive Crisis: The April–May 2018 Eruption of Piton de La Fournaise, *Ann. Geophys.* 61, <https://doi.org/10.4401/ag-7972>
- Harris, AJL., Rowland, SK. (2001), FLOWGO: A Kinematic Thermo-Rheological Model for Lava Flowing in a Channel. *Bull. Volcanol.* 63: 20–44. <https://doi.org/10.1007/s004450000120>
- Lomax, A., Virieux, J., Volant, P., & Berge-Thierry, C. (2000), Probabilistic earthquake location in 3D and layered models. In C. H. Thurber & N. Rabinowitz (Eds.), *Advances in Seismic Event Location, Modern Approaches in Geophysics* (pp. 101–134). Springer, Dordrecht, Netherlands
- Murphy, D., Bertiger, W., Hemberger, D., Komanduru, A., Peidou, A., Ries, P., & Sibthorpe, A. (2024), Jet Propulsion Laboratory Analysis Center Technical Report 2024. In R. Dach & E. Bockmann (Eds.), *International GNSS Service Technical Report 2024 (IGS Annual Report)*, IGS Central Bureau and University of Bern; Bern Open Publishing. <https://doi.org/10.48350/191991>
- Nikkhoo, M., Walter, T. R., Lundgren, P. R., & Prats-Iraola, P. (2016), Compound dislocation models (CDMs) for volcano deformation analyses, *Geophysical Journal International*, 208, 877–894
- Rebischung, P., Altamimi, Z., Métivier, L. et al. (2024), Analysis of the IGS contribution to ITRF2020, *J Geod* 98, 49. <https://doi.org/10.1007/s00190-024-01870-1>
- SeisComP (2024), SeisComP 6 – Earthquake Monitoring Software, <https://www.seiscomp>



Acknowledgments

Thank you to organizations, communities and associations for publicly posting this report for the widest dissemination

Information

All information on the Piton de la Fournaise activity can be found on the OVPF-IPGP media:

- Internet website : ipgp.fr/fr/ovpf/actualites-ovpf
- Bluesky : [@ovpf.bsky.social](https://bsky.app/profile/ovpf.bsky.social)
- Facebook : [facebook.com/ObsVolcanoPitonFournaise](https://www.facebook.com/ObsVolcanoPitonFournaise)

A preliminary automatic daily bulletin of the OVPF-IPGP, relating to the activities of the day before, validated by an analyst, is published daily. It can be accessed directly at this link:

http://volcano.ipgp.fr/reunion/Bulletin_quotidien/bulletin.html

The seismicity validated in continuous by OVPF-IPGP can also be followed on the RENASS portal: <https://renass.unistra.fr/fr/zones/la-reunion>

The OVPF-IPGP data are distributed by the IPGP data centre - Volobsis - and are also available on the EPOS and Epos-France websites ([doi:10.18715/REUNION.OVPF](https://doi.org/10.18715/REUNION.OVPF)).

The information in this document may not be used without explicit reference.